

Electrochemically and Mechanically Regulated Liquid Metal Gate via Giant Surface Tension Alteration

Yang Wang, Jiarui Guo, Yunnan Fang, Guanxiang Pang, Jingxi Wang, Xinpeng Wang, Caicai Jiao, Xuanqi Chen, Kang Sun, and Liang Hu*

Liquid gates can provide an effective method to control the release of substances. However, the size of liquid gates and the control methods limit their broad applications. The controllable large deformation of liquid metals (LMs) makes it possible to be used in liquid gate design with simple actuation methods. Here an LM gate that can be easily driven under moderate conditions is proposed, on demand opening at mild electrical voltage (2–5 V) and closing at an oscillating mechanical force (≈ 0.05 N) in a wide range of pH (2–12). The gating mechanism relies on the large surface tension alteration at these conditions, which directly changes the shape of the LM from a flat film to a contracted meniscus to one side of the copper gate-frame. As demonstrated, this gate can be applied to release substances such as liquid (ink), biomolecule (insulin) by free diffusion. Moreover, single-channel and multi-channel gates can be realized for high throughput control. The biocompatibility of the whole gate is also proved by cytotoxicity assays. Above all, a novel LM gate is offered with simple structure and easy control, which may bring inspiration to applications in controlled substance release and separation.

simple but sophisticated depending on the activation factors such as the pressure,^[4] electrical potential,^[5] and intermolecular forces at both sides of the gates. For mesoscopic gates at millimeter or centimeter scales, however, the gate control strategy options are limited. For example, active drug release gates require complicated mechanical structures, which are usually very expensive. The size constrains their structural complexity when considering the mechanical gating methods while common liquids are not proper to reversibly seal and open the gates at such sizes due to the low surface tension of most liquids. The on-demand control of mesoscopic gates with simple and effective strategy can realize the substances transportation at larger size or higher throughput, which is still of great value to pursue.

The biological world is always full of inspirations. Cell membrane can be seen as a gate, which allows transport into cell of essential nutrients and movement from the cell of waste products.^[6] In the field of bioengineering, to deliver DNAs or drugs into the cells, electroporation is an effective way to open holes on the cell membrane, basically made up of phospholipid.^[7] The cell membrane can be self-healing to seal the holes owing to the good fluidity of the phospholipid membrane.^[8] Inspired by flowing cell membrane, liquid gate with electrical control is emerging to the surface. Liquid gate based on porous membranes has been proposed by Hou et al., which has abundant and reliable applications in the fields of substance transportation and separation,^[9] controlled drug release.^[10,11] But due to their tiny pores, the transportation efficiency of the substance transportation will be relatively low. More importantly, the opening of the liquid gate depends passively on the pressure from the injection of the multiphase mixtures,^[4] which is constrained in broaden applications. Moreover, pump devices are required, which increase the complexity of the whole gate system. In this context, a liquid gate with active control, simple structure, high throughput and high efficiency is in demand.

Gallium-based eutectic alloys such as GaIn and GaInSn^[12,13] in terms as liquid metal (LM) are a group of metals with low melting points (lower than 29.8 °C melting point of pure gallium),^[14] large surface tension,^[15] and high conductivity.^[16,17] LM has been widely applied in flexible antennas,^[18–20] functional composites,^[9,21,22] 3D printing,^[16,23] flexible robots,^[24–26] etc. In

1. Introduction

Gate is a broad concept which has diverse forms ranging from the macroscopic doors to the micro/nanopores or channels. The basic function of a gate is to on-demand control the substance in and out, which has been applied in wide fields such as architecture, electrical circuits, biological organ, and cells. The control strategy of these gates and their corresponding constructions can vary based on their sizes. For macroscale gates, large and complicated systems such as pneumatic,^[1] electrical,^[2] and mechanical equipment are applied to actively control the gate. For micro- to nanoscale gates such as nanopores or channels, the gates are usually sealed by liquids.^[3] The strategies are

Y. Wang, J. Guo, X. Wang, C. Jiao, X. Chen, K. Sun, L. Hu

Beijing Advanced Innovation Center for Biomedical Engineering
Beihang University

Beijing 100191, China
E-mail: cnhliang@buaa.edu.cn

Y. Wang, J. Guo, Y. Fang, G. Pang, J. Wang, X. Wang, C. Jiao,

X. Chen, K. Sun, L. Hu

School of Biological Science and Medical Engineering
Beihang University
Beijing 100191, China

 The ORCID identification number(s) for the author(s) of this article can be found under <https://doi.org/10.1002/admi.202100954>.

DOI: 10.1002/admi.202100954

addition to the conductivity and flexibility of the LM,^[27,28] its giant deformation induced by surface tension alteration has attracted much attention especially from fluids physics, soft and smart actuation, flexible electronics,^[29,30] and nanofabrication.^[26,41] The LM surface can be easily oxidized in air or water, with its surface tension decreasing.^[19] While the surface oxides can be reduced and the surface tension regains at reducing potentials.^[12,31] In this way the flatten shape of LM contracts to a more spherical one,^[32,33] which can be utilized as gating mechanism. In addition, LM with little toxicity is widely used in biomedical applications such as drug delivery^[15,26,28] and new methods of killing cancer cells.^[17,34,35] All these LM characteristics make LM possible to manufacture an LM gate.

In this study, we propose an LM gate regulated by surface tension alteration, which enables quick open at a reducing potential and close at a mechanical shake. Taking advantage of the stable adhesion of LM on copper via intermetallic compound formation (CuGa_2), a round copper-framed round gate with one or multiple channels controlled by LM deformation is also designed. Specifically, LM gate can work under the application of moderate electrical voltages (2–5 V), which suggests its potential wide applications for material release or transportation. More experimental details are discussed as follows.

2. The Design of the LM Gate

This working setting of the LM gate is illustrated in Figure 1a. As the shape of the LM can be altered electrochemically, we utilize this principle to achieve the open of the LM gate. Ga can easily form intermetallic compounds with Cu (CuGa_2), LM can adhere to the Cu intensively.^[28] A special LM motion control

can be realized in a conductive solution at a reducing potential. We utilize this strong adhesion to fix LM on the inner circumferential surface of the copper ring. Specifically, we designed a narrow defect at the inner side of the copper ring which blocked the contact between Cu and LM by coating a narrow strip of paint (Figure 1a). Then we placed a droplet of LM in contact with the ring to wet the inner side and seal the hole as a film. Even so, the LM film still had a gap to the copper at the defect part. In this case, the whole gate was immersed in 0.9% NaCl solution which provided the conductive environment. We assume the surface tension increasing could lead to imbalanced contraction of the LM film to reveal a hole like the gate open. Originally, the LM appeared a flat film with obvious surface oxides that covered the whole ring. Under the application of a reducing potential (2 V), the surface oxide layer of the LM was reduced with its surface tension sharply increased. Then the LM film started to contract (Figure 1b,c). At the wetting part where LM stuck to the copper ring, LM maintained motionless. While at the gap where LM did not contact the copper, LM tended to contract due to the surface tension increase. In this way, the LM film contracted toward the fixed part and exposed a hole through the copper ring. Figure 1d–f demonstrates the opening process of the LM gate. Figure 1g describes the relationship between the change of the open area and time upon the application of the potential to the LM film. Notably, there is a time lag between the application of the reducing potential and the start of LM motion. During this time lag, it is observed that the dull LM surface became bright and shiny, which indicates the removal of the surface oxide. This detail is also consistent with our assumption that the surface tension increase due to the removal of its oxide leads to the LM film retraction in the opening process.

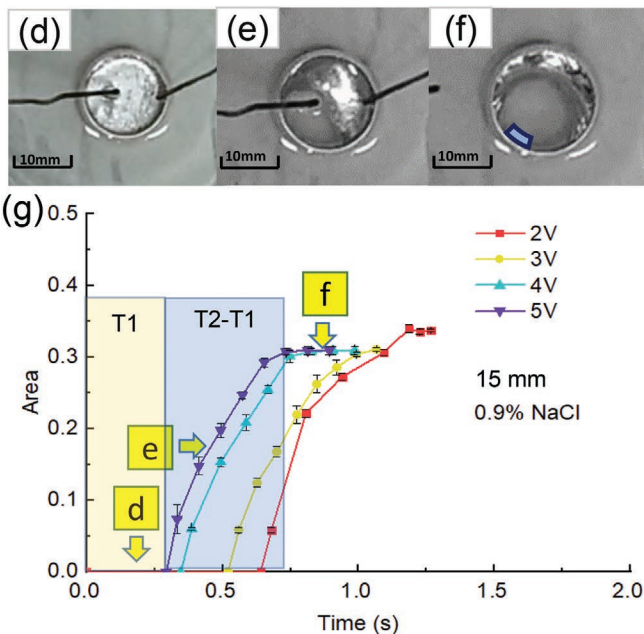
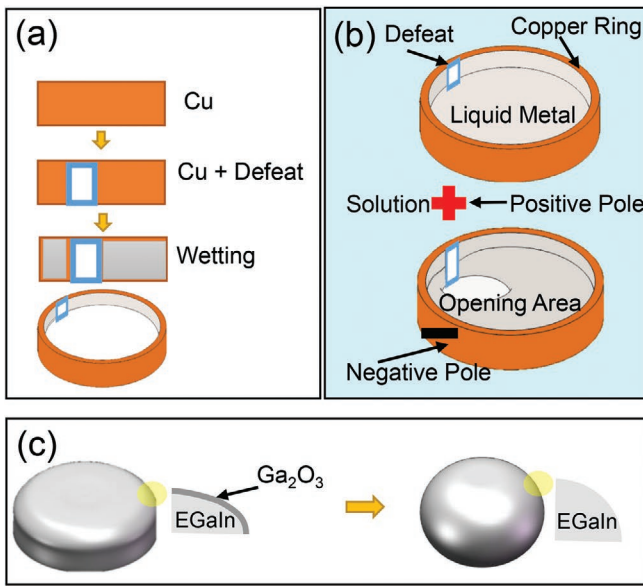


Figure 1. The design of the LM gate. a) The schematic setting of the LM gate regulated by surface tension alteration. b) The copper ring is directly connected to the negative electrode to provide the reducing potential. The positive electrode is placed in other part of the conductive solution. c) The oxide layer of LM was removed by reduction potential. d–f) The open process of the LM gate. g) The opening area of the LM gate with 15 mm diameter in 0.9% NaCl is measured at different times during the process.

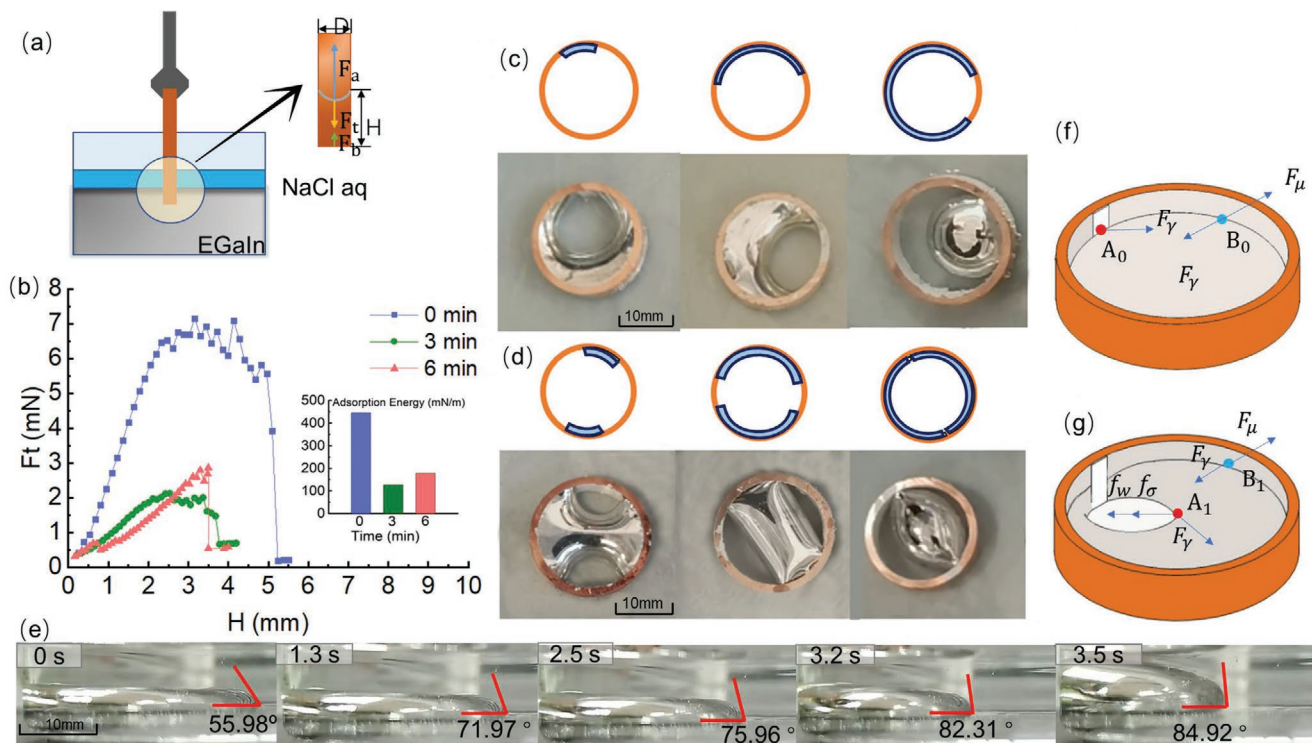


Figure 2. Wetting force between copper and LM, the shape of the LM gate and force. a) Test for wetting force between copper rod and LM. b) The tensile force between the LM and the copper rod is tested at different time, the inserted graph is the calculated adsorption energy. c) single-channel LM gate could form different shapes determined by the length of mechanical defect. d) The shape of the dual-channel gate could also be changed with the length of the mechanical defect. e) The motion of an LM drop with one side fixed to Cu foil. f,g) Force analysis of LM moving from the defect.

The opening process of this LM gate is further investigated and characterized here. During the process, the adhesion between LM and copper through CuGa₂ provides a frame for the LM motion. The CuGa₂ had a layered structure as demonstrated by scanning electron microscope (SEM) and X-ray diffraction (XRD) tests (Figure S1, Supporting Information), which was reported in previous studies.^[28,36] Here we evaluated the adhesion between LM and CuGa₂ as shown in Figure 2a. A copper rod with a diameter of 5 mm was immersed and wetted in the LM in 0.9% NaCl solution, as shown in Figure 2a. We slowly pulled up the copper rod. The rod was completely wetted with liquid state metal, which suggested the adhesion force between LM and CuGa₂ was larger than the surface tension of LM. It could ensure the resistance of the contraction tendency during the increase of surface tension.^[28,36] The maximum tensile force here mainly indicated the surface tension of the LM (maybe with surface oxide), which were measured at different time points after the reducing potential was applied. As shown in Figure 2b, the maximum tensile force could reach about 7 mN (adsorption energy 445.64 mN m⁻¹) immediately after the application of the reducing potential (0 min). As time went on, the maximum tensile force decreased as the surface oxide gradually increased. The LM gate was lying horizontally on the plate where the gravity of the LM had little influence of this open process. In order to verify that the LM gate can be used for nonhorizontal planes, we put the model on a 20° slope for operation, which could achieve normal functions in Figure S2 in the Supporting Information. If the operating environment was more complicated, a up and

down encapsulation structure with small holes can be added to hold the LM and allow the substance to pass through.

The opening process of the LM gate is caused by the LM oxide layer reducing potentials. In the environment of sodium chloride solution, LM can be slowly oxidized by slightly dissolved oxygen in the solution to form a Ga₂O₃ oxide layer.^[12] This oxide layer is about 1–3 nm.^[37] After we put the LM into the prewetted copper ring with mechanical defects, we successfully controlled the shape of the LM to form a hole like agate by adding a reducing potential. When the copper ring was externally connected to the negative electrode and the solution was connected to the positive electrode, the surface oxide layer of the LM was reduced, the surface tension was rising sharply. The LM deformed under the combined action of surface tension, gravity, resistance, and the wetting force between LM and copper until the force was balanced. The LM moved from an unfolded shape to a crescent shape.

In the research process, we made different numbers of defects on the copper ring so as to realize the functions of single-channel, double-channel, and three-channel LM gates. As shown in Figure 2c, when the defect occupied 10% of the copper ring, after the LM gate was opened, the LM was tightly combined with the copper ring at 90%, showing a crescent shape. There was no LM infiltration at the defect and the CuGa₂ layer could provide a wetting force to keep the LM “sticky” on the copper ring. When the defects account for 30% and 75%, the shape of the LM gate after opening shown in Figure 2c was different from 10%. The LM gate could form a double-hole

structure after opening if there were two symmetrical defects, as shown in Figure 2d. When there were three defects, a three-hole structure could be formed as shown in Figure S3 in the Supporting Information. Moreover, its shape was determined by the size of the defect. When a mechanical defect existed, the LM gate would open from the defect and finally formed a stable shape. We found that when the defect was relatively small (<5 mm) in the case of dual-channel and three-channel design, the LM gate would open only at one defect, as shown in Figure S3 in the Supporting Information, the dual-channel and three-channel gate ignored some of the defects and formed a shape similar to a single channel gate.

Since the LM and the copper ring were tightly connected with low resistance, they could be regarded as an equipotential surface to form a metal electrode with a special structure. Based on our theoretical analysis, the surface tension increase should be the driving force for the LM film contraction. In order to describe this movement process more vividly and accurately, we fixed one side of the LM with copper foil and drove it at a reducing potential, as shown in Figure 2e. During the movement, the left side of the LM was fixed. The right side was shrunk to the left side, where the contact angle between the right side and the substrate continued to increase. At the beginning, the LM was in the solution with an oxide layer on its surface. The contact angle between the LM and the substrate was 55.98°. As the LM contracted, the contact angle finally increased to 84.92°, reaching a stable state. When the LM was fixed in the copper ring, this movement trend was similar. The LM would contract inward from the defect. The increasing contact angle demonstrated the surface tension increase during the contraction. The mechanic analysis during the LM gate open from a single point defect is carried out as shown in Figure 2f,g. At the beginning, the oxide layer of the LM was removed. At A₀ in Figure 2f, it was subjected to surface tension and gravity, so it shrank inward. At B₀ without defect, although there was a shrinkage tendency caused by surface tension, it was not enough to overcome the wetting force between LM and Cu. The LM at point B₀ did not move. During the movement in Figure 2g, A₁ was subjected to frictional resistance, fluid resistance, surface tension as the driving force, and gravity. At points B₁ that were in contact with the copper ring, they were subjected to surface tension, wetting force, and gravity.

3. The Control Parameters of the LM Gate

The factors that affect the dynamics of LM gate opening process are examined and evaluated. The speed of opening process should be positively related to the reducing speed of its oxide layer on the surface, which is mainly depend on the magnitude of the applied voltage, the conductive ion concentration, and pH of the solution. Generally, the higher the voltage is, the faster the LM gate opens. When the concentration of the solution rises, the electrical conductivity is increased and the opening speed will be faster. In acidic and alkaline conditions, the LM gate opens faster than in neutral conditions. The height of the copper ring nearly has no effect on the opening process of the LM gate.

From the experimental observation and the curves, we could conclude that the opening process could be divided into two parts: the motionless state with surface oxide layer being reduced, the opening motion state. The time from the electricity supplied to the time when the LM started to move was recorded as T1. The time that the LM gate was fully opened was recorded as T2. T2-T1 represented the time that the LM gate took during opening. T1 and T2-T1 could be clearly seen in Figure 1g. T1 and T2-T1 can concretely describe the reduction rate of LM oxide layer.

In Figure 3a, the relationship between T1 and different voltages of LM gate with different diameters was described. With the voltage increased, T1 decreased gradually. This was due to the increase of voltage facilitate the removal of the surface oxide. Another phenomenon was that under the same voltage, T1 decreased regularly with the model diminishing in size. The reason was the increase area of LM surface oxide that requires more time for reduction.

As shown in Figure 3b, we studied the moving time of the LM in relation to the voltage and found that it only took less than 1 s to complete the opening process after the oxide layer was removed. When the diameters were 20 and 25 mm, the T2-T1 value decreased with the voltage increasing, indicating that the LM moved faster. When the diameters were 9 and 15 mm, the correlation between T2-T1 value and voltages was not obvious. One possible reason was that the change of small LM droplet surface charge distribution gradient was not obvious at small voltage after the LM oxide layer was reduced.

The relationship between the solution concentration and the time T1 of removing the oxide layer was examined as shown in Figure 3c. When the concentration increased, the time T1 for removing the LM oxide layer was shorter, which was the similar trend for the different diameters. The conductivity of the solution was affected by the ion concentration. With the ion concentration increased, the conductivity of the solution became higher and the oxide layer of the LM was removed faster.^[38] The LM gate with larger size had larger T1. This was caused by the larger area of the oxide layer on LM surface. In 0.15 and 0.2 mol L⁻¹ solution, the law was obvious. But when the concentration was 0.4 and 0.6 mol L⁻¹, the difference caused by different sizes was very small because the movement speed was too fast.

Figure 3d described the relationship between the LM moving time T2-T1 and the concentration under different diameters. With the increase of concentration, the moving speed of the LM went up significantly. The potential gradient between the LM interface and the solution interface became larger, which would speed up changing the surface tension of the LM, accelerating the movement of the LM.^[39,40] Under the same concentration, theoretically the larger the diameter, the longer the moving time, but in the actual test process, we found that there was no obvious law between the diameter and the moving time.

Different aqueous environments will affect the change of LM surface tension, which has been previously reported by scholars.^[20] Considering that liquid gates may be applied in different scenarios, the working situation of liquid gates in different pH is also discussed in this study. As shown in Figure 3e, we discussed the influence of pH on the opening speed of the LM gate. When the pH was 1, 13, and 14, we noticed that the

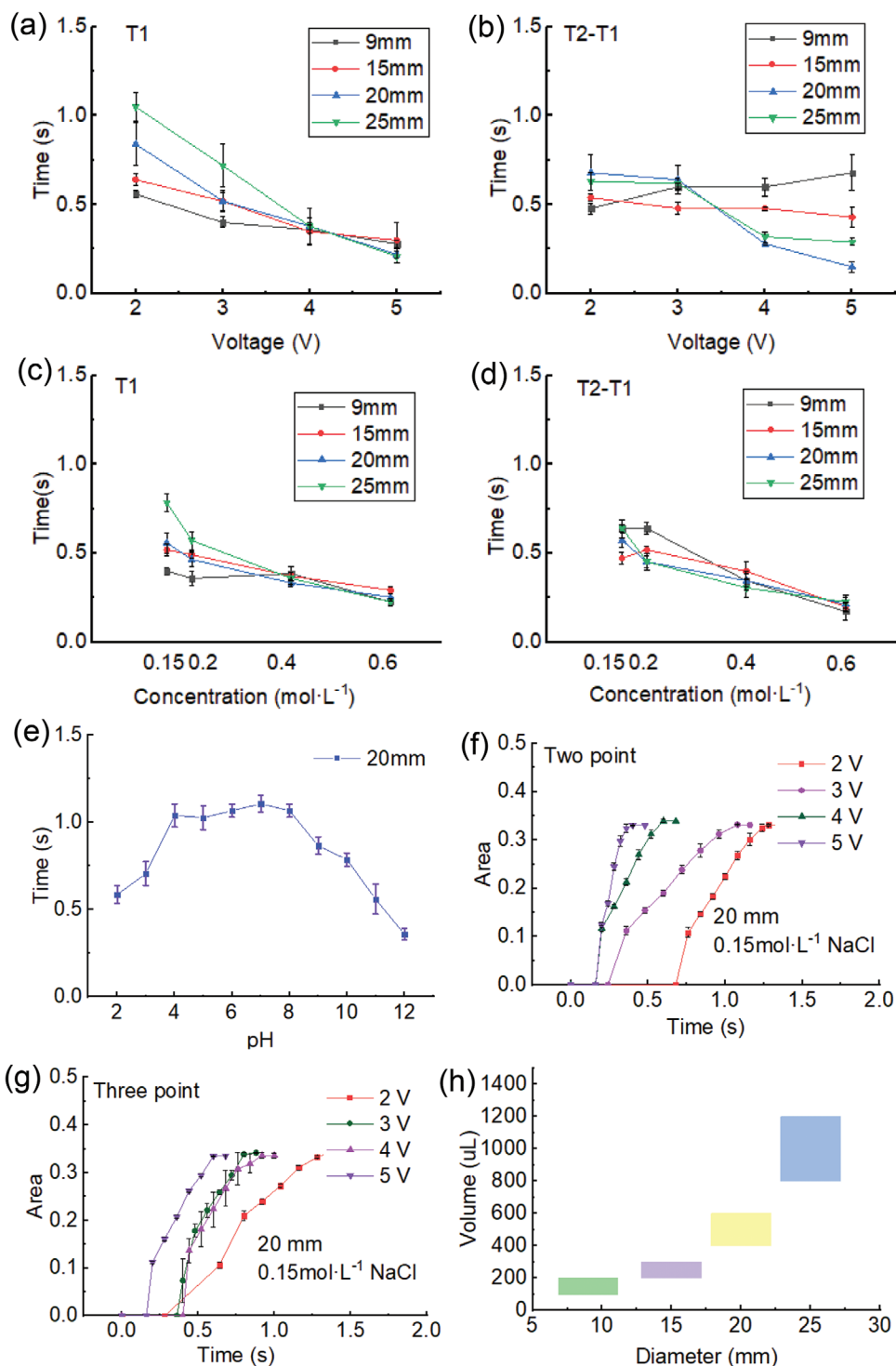


Figure 3. Control parameters for the opening of the LM gate. a) Time of starting moving under different voltages and diameters. b) Time of keeping moving under different voltages and diameters. c) Time of starting moving under different NaCl concentration and diameters. d) Time of keeping moving under different NaCl concentration and diameters. e) The time that the LM gate opened took in different pH solution. f) The process that the dual-channel LM gate opened at different voltages. g) The process that the three-channel LM gate opened at different voltages. h) The volume of LM required for the models of different diameters.

LM gate could not be closed. With the increase of pH, the opening time of the LM gate first increased and then decreased. When pH was 4–8, the time was approximate, but longer.

When the pH was larger than 9, the time decreased rapidly. The pH affected the opening time of the LM gate because there was a difference between the rate of formation and removal of

the oxide layer in acid and alkali. If the pH was too small or too large ($\text{pH} = 1, 13, 14$), the formation speed of the LM oxide layer was smaller than removal speed, so the LM gate could not work properly. The closer the pH was to neutral, the slower the removal rate of the LM oxide layer was. In this experiment, we observed that alkaline was more conducive to removing the oxide layer of LM than acid, so the time it took was shorter. The opening rules of dual-channel LM gate and three-channel LM gate are similar to that of single channel, as shown in Figure 3f,g. When the voltage became larger, the speed of the gate opening became faster. This law was consistent with the single-channel LM gate.

In addition, we conducted experiments related to the opening of the LM gate corresponding to 9, 15, 20, 25 mm, and the volume of LM. The volume of LM matching 9 mm diameter model was 100–200 μL . When the volume of LM was too large, the area that the gate opened would be smaller, which would affect the working efficiency of the gate. If the volume of LM was too small, it was difficult to close. The specific data of the four different diameters corresponded to the working volume is shown in Figure 3h.

During the experiment, we found that the height of the copper ring had no obvious effect on the operation of the liquid door. In fact, whether the LM gate could work normally was determined by the thickness of the liquid metal layer. The thickness was matched by the volume of the liquid metal and the diameter of the model. Taking the 9 mm model as an example, the volume of LM was 150 μL . Under the same liquid metal volume and diameter, we used white paint to construct different internal wetting layer heights (2, 3, and 5 mm) to instead of different copper ring heights to insure the copper ring could hold the LM. The experimental results were shown in Figure S4 in the Supporting Information. There was no effect on the opening shape, and at the same time, the difference in opening speed was not obvious. T1 and T2-T1 was similar in different groups.

Square waves and sine waves with a period of 20 s were also used to test the opening of the LM gate.^[41] When the amplitude was greater than 3 V, it could be opened successfully (Movies S1 and S2, Supporting Information). Unfortunately, it could not be closed by electrical stimulation. Although the formation of the oxide layer could be accelerated at oxidation potential, the surface tension gradient did not generated in the neutral solution, so the LM nearly had no deformation and movement. At the time the LM was connected to the reduction potential, it moved and the liquid gate opened. As the reduction potential changed to the oxidation potential, the LM surface lost its metallic luster and got darker without any obvious movement.

Through the acceleration movement, the relative displacement of the LM interface and the water environment interface would accelerate the production of the LM oxide layer on its surface. The oxide layer was so fragile that it was easily broken under the action of acceleration, by the time the exposed LM quickly renewed the oxide layer. As the oxide layer increased, the surface tension of the LM rapidly decreased, and the LM was unable to maintain the tendency of shrinking. The LM spread out to form a reliable liquid seal under the restriction of the copper ring and its own gravity. From the phenomena we successfully closed the LM gate (Movie S3, Supporting

Information). We considered the closing time was affected by the breakage and generation of the liquid metal oxide layer, which controlled by the acceleration of the reciprocating motion and the volume of the liquid metal.

A horizontal reciprocating shaker was used to quantify the inertial force applied to the close process. Figure 4a is a group of photos shown the closing process on a reciprocating shaker, in which the opening area was becoming smaller and soon totally closed. In fact, in the closing process, the volume of LM and the acceleration of the horizontal reciprocating shaker were the decisive factors. In Figure 4b, the diameter of the gate was 9 mm, the abscissa was the rotation speed of the shaker and the ordinate was the time required for the gate to close. Each point represented the time required for the gate to close at this speed. We could know that for a curve with the same volume of LM, the larger the speed, the shorter the time required for the gate to close. When the volume was 100 μL and the speed was 200, 210, and 220 r min^{-1} , the average closing time is 45.12, 34.17, and 20.70 s. At the same speed, the closing time would be shorter with the volume of LM gained. When the speed was 200 r min^{-1} and the volume was 100, 150, and 200 μL , the corresponding time was 45.12, 43.46, and 34.78 s. In fact, if the movement was irregular, such as shaking with the hand, it only took 10 s to close (Movie S4, Supporting Information).

Figure 4c–e corresponded to the experimental results of 15, 20, and 25 mm diameters, respectively. The law was the same as at 9 mm. From this we believe that the closing time of the gate was mainly related to the volume of LM and the speed of the shaker. The larger the volume, the higher the shaker speed, and the shorter the time would take.

Due to the wetting force of LM and copper, the LM and the gate could be tightly connected. When the gate was opened, the inertial force generated by the mechanical shaking could reclose the LM gate. The equation of motion for a horizontal reciprocating shaker was: $x = A \cos(\omega t + \phi)$. Acceleration equation was: $a = A\omega^2 \cos(\omega t + \phi + \pi)$. Where x was the horizontal position, A was the amplitude, ω was the angular velocity, and ϕ was the initial phase. F was related to the quality of the LM and the acceleration that the shaker could provide. Equation of inertial forces was $F = -ma$.

Take the 9 mm model as an example, the speed of 190 r min^{-1} , the amplitude of 5 cm, and the liquid metal volume of 100 μL were taken into the calculation, The final result was $F = 0.012 \text{ N}$. Theoretically, when the mass of the LM increased, the closing effect of the gate became better when the acceleration provided by the shaker increased.

4. Application and Cytotoxicity Test

The LM gate has potential application in substance delivery, drug release and other directions. To verify its release effect, we demonstrated it with ink and quantitatively tested it with insulin. We used single-channel and three-channel LM gates to demonstrate ink release experiments to prove that this model can be used for controlled release of substances. As shown in Figure 5a, the gated part composed of copper ring and LM was put on top of the cavities model, filled with ink in the cavities. When voltage was applied, the LM gate was opened, and the

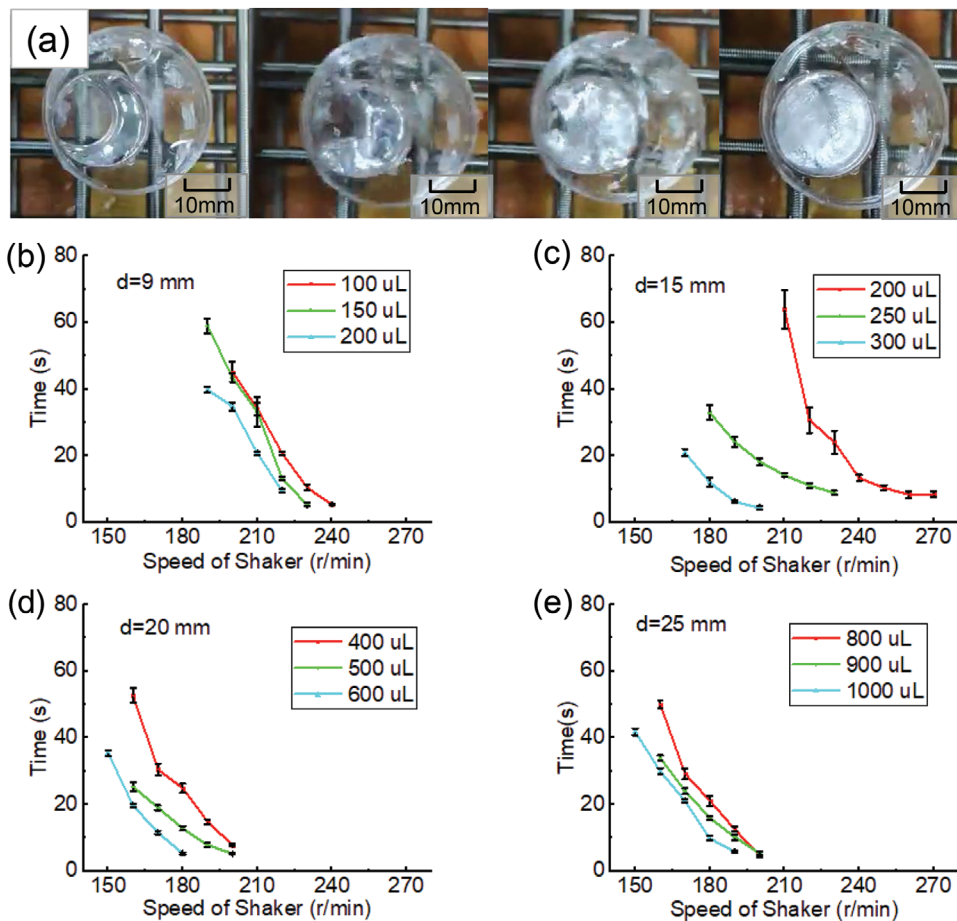


Figure 4. The closing process and parameters of the LM gate. a) A group photo of the LM gate closing on the shaker. b–e) The closing time of four diameters LM gates with different volumes at different shaking speeds.

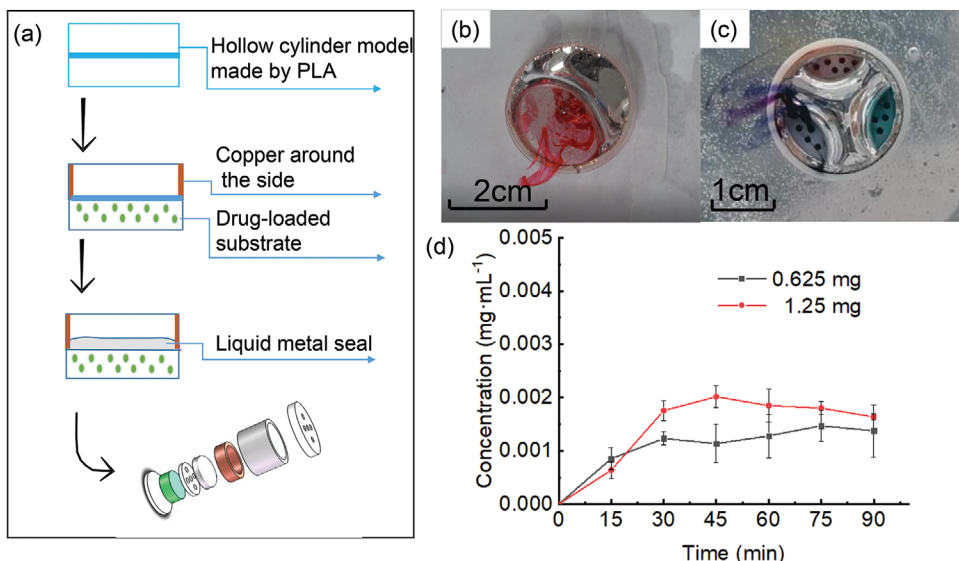


Figure 5. Applications of the LM gate. a) The outer scaffold was 3D-printed by polylactic acid (PLA) and combined with copper ring and LM to form a substance release controlled model. b) Single channel LM gate control the release of ink. c) Three channel LM gate control the release of ink. d) Single channel LM gate control the release of insulin.

ink quickly escaped from the below. In the model of single-channel LM gate, the red ink quickly released when the gate was open as shown in Figure 5b. The three-channel model with three independent reservoir chambers also proved its function that three colored ink can be released from each chamber in Figure 5c, which suggest its further application in multiple substance control and release. The complete showcase is available in Movies S5 and S6 in the Supporting Information. As demonstration, we applied this model to the controlled release of insulin. The single-gate model was used for quantitative release testing, where the insulin solution was placed in the below cavity. The insulin solution (50 and 100 μL , 12.5 mg mL^{-1}) was put in the cavity below the LM gate and was released in 100 mL physiological saline. As shown in Figure 5d, insulin was released quickly after the gate was turned on and it showed an increasing trend within 45 min.

We have proved that this LM gate can function in normal saline as aqueous solution, which suggests its feasibility in physiological environment. To prove that it has potential in biomedicine as well, we examined the biocompatibility of this LM gate. We cultured mouse fibroblasts (NIH-3T3) to test cytotoxicity of LM and other materials in vitro, the low toxicity characteristics of LM was initially verified. As shown in Figure S7 in the Supporting Information, after the cells had adhered to the wall for 24 h in 12 well plate, we added materials into different groups. The metal in the cell experiment was in direct contact with the solution. The survival rate of the blank group was 86%, the cell survival rate of the Cu-LM group was 75%, and the cell survival rate of the LM group was 87% shown in Figure 6a. The toxicity of the blank group was similar to that of the LM group. The cell photos of three groups were shown in Figure S7 in the Supporting Information. In the cell group, it could be observed that the cells grow adherent normally and a small number of dead cells were dyed blue by trypan blue. The number of dead cells has increased in the Cu-LM group and some of the cells were spherical, indicating a poor growth state. The cell growth of the LM group was similar to that of the cell group. Through analysis of variance, there was no significant difference between the cell group and other two groups. In fact, our drug-loaded model was wrapped by a layer of polylactic acid, which further reduced the possibility of direct contact between metal and bio-

logical tissues. This means that it is possible for us to apply the drug-loaded controlled-release model to the human body.

5. Conclusion

In the present study, a liquid metal gate is introduced with the advantages of on-demand control, fast response, and high throughput. The giant deformation of the liquid metal achieves the open and close of a copper-framed gate under the application of moderate electrical voltages (2–5 V) and oscillating mechanical force (0.05 N) in wide pH ranges, respectively. The simple structure together with easy control provides great promise in substance release and separation devices. The control parameters are examined and the results show that the time of the LM gate opening is positively related to the solution concentration and voltage; the time of the LM gate closing is positively related to the volume of the LM and the magnitude of the inertial force. The controllable release of the ink and insulin through this LM gate together with its biocompatibility suggest the feasibility and great potential of this LM gate in controlled drug release stents and other biomedical devices. Moreover, the multichannels design can achieve multiple substances release, which may further enhance the capacity of this gating system.

6. Experimental Section

Materials: Gallium and indium were purchased from Mai Xi company, Shanghai, China. Gallium (75%) and indium (25%) were heated and melted at 60 °C to produce eutectic alloy LM. Copper rings were purchased from Xin Cheng Metal-Material Company, Shenzhen, China. Other chemical drugs were purchased from Sinopharm Group Chemical Reagent Co., Ltd. Polylactic acid shell was produced by Chicheng 3D printing company. 0.4% Trypan blue dye was purchased from Phygene Company.

Fabrication of Wetting Layer between Copper Ring and LM: After sanding the copper ring with sandpaper, it was place in 0.1 mol L^{-1} hydrochloric acid, and LM droplet was added, to form a CuGa_2 wetting layer on the copper ring with a negative voltage of 3 V. Redundant LM was removed and white paint was used to form a mechanical defect on the wetting layer.

Substance Controlled Release Model: The model had a top and below part, made of polylactic acid by 3D printing. The top part was fixed with the processed copper ring and the below part was used for placing drugs or other substances.

Characterization of LM Oxide Layer and CuGa_2 : The oxide layer on the surface of the LM and the infiltration of the LM and copper were characterized by electron microscopy SEM from Beihang University. The oxide layer on the surface of the LM is formed by placing it in a 0.15 mol L^{-1} sodium chloride solution for 5 min, and removing the oxide layer with tweezers. LM and copper are infiltrated in 0.1 mol L^{-1} hydrochloric acid, using 8 mm × 8 mm copper foil, and 2 mL of LM. After 5 min of infiltration, the LM and liquid residue are washed away, and the copper foil is taken out. Flatten the removed sample and paste it on the electron microscope sample table with conductive adhesive for testing.

Wetting Force Measurement: A 5 mm copper rod was extended into LM in the 0.15 mol L^{-1} sodium chloride solution for 3 mm, the force was measured when the copper rod was pulled up, and the wetting force was calculated. The test instrument is a surface tension tester, provided by the Institute of Physical and Chemical Technology, Chinese Academy of Sciences.

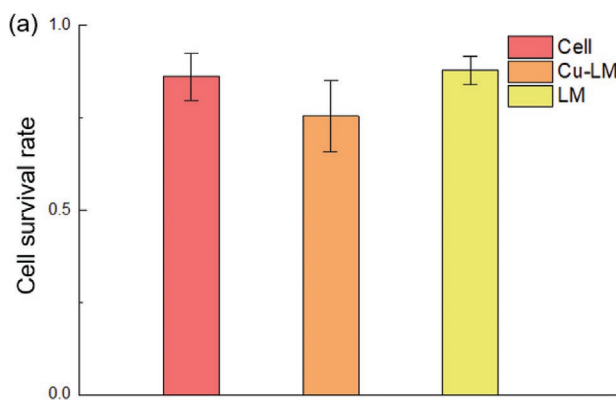


Figure 6. Cytotoxicity results. Cell survival rate of Cell, Cu-LM, and LM group.

Opening Experiment of the LM Gate: In order to obtain the conditions for the stable opening of the control gate, a simplified design was adopted when the gate was open, and the copper ring part was only used for the gate experiment. A defect was made on the copper ring and LM wetted wall surface to improve the effect of opening the gate. The copper ring and LM were put into a solution environment for experiments, an external voltage was the power to turn on the gate, and the process was recorded by a high-speed camera. The potential distribution of the solution environment after applying 3 V voltage to the LM gate model in a 0.15 mol L⁻¹ NaCl solution was described in Figure S5 in the Supporting Information.

Closing Experiment of the LM gate: In order to study the process of close, a horizontal reciprocating shaker was used to provide horizontal inertial force. By changing the speed of the shaker, the diameters of the model, LM volume, the time required for the gate to close was different.

Ink Release Experiment: In order to verify the tightness and controllability of the gate, ink was chosen as the developer and the ink was placed under the LM gate. Whether the gate was off could be seen through the flow of ink. If the gate was turned on, the ink was to spread.

Insulin Release Experiment: The rate of insulin release in vitro was studied. The insulin solution was put in the cavity below the LM gate and was released in 100 mL physiological saline. 500 μL sample was taken per 15 min. Coomassie Brilliant Blue solution was added at a ratio of 1:5. After dyeing, the absorbance of the sample with a UV spectrophotometer was measured at a wavelength of 595 nm. The insulin concentration in the solution was obtained by comparing the absorbance with the bovine serum protein standard curve.

Bovine Serum Protein Standard Curve: 2500 μL Coomassie brilliant blue solution was added into 500 μL sample for staining after preparing 0.002–0.01 mg mL⁻¹ bovine serum albumin solution. The absorbance was measured with UV spectrophotometer at 595 nm wavelength and concentration-absorbance curve was shown in Figure S6 in the Supporting Information. The standard curve equation is $y = 14.064x$, $r^2 = 0.98$.

Cell Experiment: The NIH-3T3 cells were passaged in a 12-well plate at a density of 8000 cells per well and 1 mL of cell culture medium was added. Before the materials were added, cells were cultured at 37 °C with 5% CO₂ for 24 h. Then 50 μL LM was added in the LM group. 50 μL LM and a presoaked Cu foil (3 mm × 3 mm) were added in the Cu-LM group. After adding the materials, they were incubated for another 24 h. Then the materials were removed and cells were washed with phosphate buffer saline (PBS). Trypan blue dye was added to stain the dead cells. Cell photos were recorded with a microscope and ImageJ was used to count the number of live and dead cells. There were three samples for each set group of the cell experiment.

Supporting Information

Supporting Information is available from the Wiley Online Library or from the author.

Acknowledgements

The authors thank financial support from the National Natural Science Foundation of China and Beijing Natural Science Foundation (Grant No. 7202104).

Conflict of Interest

The authors declare no conflict of interest.

Data Availability Statement

The data that support the findings of this study are available in the supplementary material of this article.

Keywords

liquid metal gates, multichannel gates, oscillating mechanical force, substance release, surface tension alteration

Received: June 9, 2021

Revised: July 4, 2021

Published online:

- [1] M. W. Li, B. H. Huynh, M. K. Hulvey, S. M. Lunte, R. S. Martin, *Anal. Chem.* **2006**, *78*, 1042.
- [2] C. J. Huang, F. T. Tsai, *Appl. Mech. Mater.* **2013**, *421*, 99.
- [3] Y. Zhang, J. Li, R. Li, D.-T. Sbircea, A. Giovannitti, J. Xu, H. Xu, G. Zhou, L. Bian, I. McCulloch, N. Zhao, *ACS Appl. Mater. Interfaces* **2017**, *9*, 38687.
- [4] Z. Sheng, J. Zhang, J. Liu, Y. Zhang, X. Chen, X. Hou, *Chem. Soc. Rev.* **2020**, *49*, 7907.
- [5] J. Zhang, K. Zhan, S. Wang, X. Hou, *Soft Matter* **2020**, *16*, 2915.
- [6] Y. Cheng, Y. Dong, Q. Huang, K. Huang, S. Lyu, Y. Chen, J. Duan, D. Mo, Y. Sun, J. Liu, Y. Peng, H. Yao, *ACS Appl. Mater. Interfaces* **2021**, *13*, 9015.
- [7] P. Mukherjee, E. J. Berns, C. A. Patino, E. Hakim Mouly, L. Chang, S. S. P. Nathamgari, J. A. Kessler, M. Mrksich, H. D. Espinosa, *Small* **2020**, *16*, 2000584.
- [8] A. Bouter, R. Carmeille, C. Gounou, F. Bouvet, S. A. Degrelle, D. Evain-Brion, A. R. Brisson, *Placenta* **2015**, *36*, S43.
- [9] X. Hou, Y. Hu, A. Grinthal, M. Khan, J. Aizenberg, *Nature* **2015**, *519*, 70.
- [10] W. Lv, Z. Sheng, Y. Zhu, J. Liu, Y. Lei, R. Zhang, X. Chen, X. Hou, *Microsyst. Nanoeng.* **2020**, *6*, 43.
- [11] W. Liu, M. Wang, Z. Sheng, Y. Zhang, S. Wang, L. Qiao, Y. Hou, M. Zhang, X. Chen, X. Hou, *Ind. Eng. Chem. Res.* **2019**, *58*, 11976.
- [12] M. D. Dickey, *ACS Appl. Mater. Interfaces* **2014**, *6*, 18369.
- [13] X. Zhao, S. Xu, J. Liu, *Front. Energy* **2017**, *11*, 535.
- [14] I. Dutta, P. Kumar, *Appl. Phys. Lett.* **2009**, *94*, 184104.
- [15] T. Daeneke, K. Khoshmanesh, N. Mahmood, I. A. de Castro, D. Esrafilzadeh, S. J. Barrow, M. D. Dickey, K. Kalantar-Zadeh, *Chem. Soc. Rev.* **2018**, *47*, 4073.
- [16] J. Shu, Y. Lu, E. Wang, X. Li, S. Y. Tang, S. Zhao, X. Zhou, L. Sun, W. Li, S. Zhang, *ACS Appl. Mater. Interfaces* **2020**, *12*, 11163.
- [17] Y. Hou, P. Zhang, D. Wang, J. Liu, W. Rao, *ACS Appl. Mater. Interfaces* **2020**, *12*, 27984.
- [18] S. Yu, M. Kaviany, *J. Chem. Phys.* **2014**, *140*, 064303.
- [19] R. K. Kramer, J. W. Boley, H. A. Stone, J. C. Weaver, R. J. Wood, *Langmuir* **2014**, *30*, 533.
- [20] A. Zavabeti, T. Daeneke, A. F. Chrimes, A. P. O'Mullane, J. Zhen Ou, A. Mitchell, K. Khoshmanesh, K. Kalantar-Zadeh, *Nat. Commun.* **2016**, *7*, 12402.
- [21] J. Tang, X. Zhao, J. Li, R. Guo, Y. Zhou, J. Liu, *ACS Appl. Mater. Interfaces* **2017**, *9*, 35977.
- [22] J. Tang, X. Zhao, J. Li, Y. Zhou, J. Liu, *Adv. Sci.* **2017**, *4*, 1700024.
- [23] A. Gannarapu, B. A. Gozen, *Adv. Mater. Technol.* **2016**, *1*, 1600047.
- [24] J. Jeon, J. B. Lee, S. K. Chung, D. Kim, *Lab Chip* **2016**, *17*, 128.
- [25] S. Chen, X. Yang, Y. Cui, J. Liu, *ACS Appl. Mater. Interfaces* **2018**, *10*, 22889.
- [26] D. Wang, W. Xie, Q. Gao, H. Yan, J. Zhang, J. Lu, B. Liaw, Z. Guo, F. Gao, L. Yin, G. Zhang, L. Zhao, *Small* **2019**, *15*, 1900511.
- [27] P. A. Lopes, H. Paisana, A. T. De Almeida, C. Majidi, M. Tavakoli, *ACS Appl. Mater. Interfaces* **2018**, *10*, 38760.

- [28] Y. Cui, F. Liang, Z. Yang, S. Xu, X. Zhao, Y. Ding, Z. Lin, J. Liu, *ACS Appl. Mater. Interfaces* **2018**, *10*, 9203.
- [29] J. Zhang, R. Guo, J. Liu, *J. Mater. Chem. B* **2016**, *4*, 5349.
- [30] I. A. D. Castro, A. F. Chrimes, A. Zavabeti, K. J. Berean, B. J. Carey, J. Zhuang, Y. Du, S. X. Dou, K. Suzuki, R. A. Shanks, R. Nixon-Luke, G. Bryant, K. Khoshmanesh, K. Kalantar-Zadeh, T. Daeneke, *Nano Lett.* **2017**, *17*, 7831.
- [31] S. Handschuh-Wang, Y. Chen, L. Zhu, X. Zhou, *ChemPhysChem* **2018**, *19*, 1584.
- [32] M. Mohammed, R. Sundaresan, M. D. Dickey, *ACS Appl. Mater. Interfaces* **2015**, *7*, 23163.
- [33] J. Chen, J. Zhang, Z. Luo, J. Zhang, L. Li, Y. Su, X. Gao, Y. Li, W. Tang, C. Cao, Q. Liu, L. Wang, H. Li, *ACS Appl. Mater. Interfaces* **2020**, *12*, 22200.
- [34] X. Wang, W. Yao, R. Guo, X. Yang, J. Tang, J. Zhang, W. Gao, V. Timchenko, J. Liu, *Adv. Healthcare Mater.* **2018**, *7*, 1800318.
- [35] L. Fan, M. Duan, X. Sun, H. Wang, J. Liu, *ACS Appl. Bio Mater.* **2020**, *3*, 3553.
- [36] S. Liu, S. McDonald, Q. Gu, S. Matsumura, D. Qu, K. Sweatman, T. Nishimura, K. Nogita, *J. Electron. Mater.* **2019**, *49*, 128.
- [37] K. Doudrick, S. Liu, E. M. Mutunga, K. L. Klein, V. Damle, K. K. Varanasi, K. Rykaczewski, *Langmuir* **2014**, *30*, 6867.
- [38] C. S. Widodo, H. Sela, D. R. Santosa, *AIP Conf. Proc.* **2021**, *1*, 050003.
- [39] J. Zhang, L. Sheng, J. Liu, *Sci. Rep.* **2014**, *4*, 7116.
- [40] M. R. Khan, C. B. Eaker, E. F. Bowden, M. D. Dickey, *Proc. Natl. Acad. Sci. U. S. A.* **2014**, *111*, 14047.
- [41] M. Mayyas, M. Mousavi, M. B. Ghasemian, R. Abbasi, H. Li, M. J. Christoe, J. Han, Y. Wang, C. Zhang, M. A. Rahim, J. Tang, J. Yang, D. Esrafilzadeh, R. Jalili, F.-M. Allioux, A. P. O'Mullane, K. Kalantar-Zadeh, *ACS Nano* **2020**, *14*, 14070.